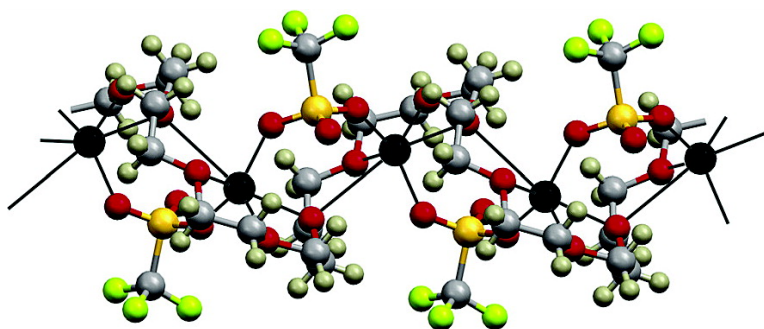


Single-Crystal Structures of Polymer Electrolytes

Wesley A. Henderson, Neil R. Brooks, and Victor G. Young

J. Am. Chem. Soc., **2003**, 125 (40), 12098-12099 • DOI: 10.1021/ja036535k • Publication Date (Web): 13 September 2003

Downloaded from <http://pubs.acs.org> on March 29, 2009



More About This Article

Additional resources and features associated with this article are available within the HTML version:

- Supporting Information
- Access to high resolution figures
- Links to articles and content related to this article
- Copyright permission to reproduce figures and/or text from this article

[View the Full Text HTML](#)

Single-Crystal Structures of Polymer Electrolytes

Wesley A. Henderson,*† Neil R. Brooks,‡ and Victor G. Young, Jr.‡

Department of Chemical Engineering & Materials Science, and X-ray Crystallographic Laboratory,
Department of Chemistry, University of Minnesota, Minneapolis, Minnesota 55455

Received June 6, 2003; E-mail: wesley.henderson@casaccia.enea.it

Solid polymer electrolytes, formed by the dissolution of salts, such as LiCF_3SO_3 and $\text{LiN}(\text{SO}_2\text{CF}_3)_2$, directly into an ion-coordinating polymer, such as poly(ethylene oxide) (PEO) $[\text{CH}_3\text{O}-(\text{CH}_2\text{CH}_2\text{O})_n-\text{CH}_3]$, form a fascinating class of coordination compounds.¹ Mobile ions in the flexible membranes create highly conductive materials which show potential for use in all-solid-state high energy batteries. The first commercial lithium–metal–polymer (LMP) battery manufacturing plant was inaugurated by AVESTOR in September 2002. These batteries use a “dry” or solvent-free polymer electrolyte membrane as opposed to the gel-polymer electrolytes used in standard commercial lithium-ion (“lithium”) batteries. LMP batteries represent the next generation of advanced energy technologies for electric vehicle, hybrid electric vehicle, and telecommunication applications.

Despite the extensive attention devoted to dry electrolytes, the mechanisms by which ions are transported through the membranes remain poorly understood. Crystalline PEO-salt phases may form in PEO electrolytes, but ionic conductivity has been shown to predominate in amorphous materials.¹ The relationship between solvate structures and ionic conductivity is largely undeveloped as structural characterization of amorphous solvates has proven to be a formidable task.² Such studies are greatly aided by crystalline solvate characterization, but this presents another set of challenges.³

Phase diagrams of PEO-salt mixtures have revealed the existence of numerous crystalline phases.⁴ The first structurally characterized PEO-salt phases were determined from stretched oriented fibers.⁵ It is difficult to prepare such samples, however, and the data interpretation tends to be problematic.⁶ In contrast, high quality powder diffraction data for polycrystalline samples are relatively easy to obtain. The first polymer electrolyte structure determined from powder data was the $\text{P}(\text{EO})_3:\text{NaClO}_4$ phase, and other structures have slowly followed.⁷ Yet once again, interpretation of the data is difficult. The combination of ab initio structural solutions with Rietveld refinement of powder data, the so-called simulated annealing technique, has been employed to determine complex crystal structures of several flexible polymer electrolyte phases.⁸ The analysis, however, is far from trivial.⁹ Single-crystal structural determination still remains the technique of choice.

High-quality single crystals of polymer electrolytes have not been available because high molecular weight PEO-salt mixtures are powders or spherulitic films when crystalline. We have approached the difficult task of polymer electrolyte solvate structural characterization in a different manner. An extensive investigation of oligomeric $\text{CH}_3\text{O}-(\text{CH}_2\text{CH}_2\text{O})_n-\text{CH}_3$ glyme-lithium salt phase behavior was undertaken.¹⁰ Numerous crystalline glyme-salt solvates form. As the glyme chains become longer, the solvate structures approach those found in PEO. It has been reported that the same PEO–LiX crystalline phases are formed with low, PEO(1000) and PEO(2000), and high, PEO(5×10^6), molecular weight

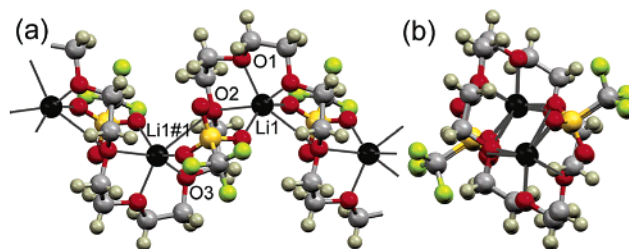


Figure 1. Li^+ cation coordination environment in the single-crystal structure of $\text{P}(\text{EO})_3(500):\text{LiCF}_3\text{SO}_3$ (Li, black; O, red; S, gold; F, green). (a) Lateral view and (b) axial view.

polymers.^{9e,f} PEO(1000) is a waxy solid with a T_m of 42 °C, while PEO(500) is a viscous liquid at 22 °C. DSC traces of PEO(500) have multiple melting peaks, indicating that the polymer is actually a mixture of different chain lengths with an average of 10–12 ethoxy segments. We have used this latter polymer to grow single crystals of polymer electrolyte phases.

The crystal structure of the $\text{P}(\text{EO})_3(5 \times 10^6):\text{LiCF}_3\text{SO}_3$ phase with high molecular weight PEO has been previously determined from powder data.^{7b} We have determined the structure of this phase from single crystals of $\text{P}(\text{EO})_3(500):\text{LiCF}_3\text{SO}_3$ (Figure 1).^{11a} The two structures are essentially isostructural. The monoclinic unit cell with space group $P2_1/n$ for $\text{P}(\text{EO})_3(500):\text{LiCF}_3\text{SO}_3$ has $a = 10.0678(16)$ Å, $b = 8.5275(14)$ Å, $c = 14.399(2)$ Å, and $\beta = 96.023(3)^\circ$, whereas the powder data $\text{P}(\text{EO})_3(5 \times 10^6):\text{LiCF}_3\text{SO}_3$ refinement gave $a = 10.064$ Å, $b = 8.613$ Å, $c = 14.441$ Å, and $\beta = 95.65^\circ$.^{7b} The principal difference between the two structures lies in the use of low molecular weight PEO to grow the single crystals resulting in the presence of terminal methyl groups. The terminal methyl groups cause apparent disorder in the PEO chains with certain ethylene links being replaced, part of the time, by two methyl groups. From the refined occupancy of these methyl groups, it is possible to calculate an average length of the single-crystal PEO chains to be close to 15 ethoxy segments (see Supporting Information).

A close examination of the ether oxygen $\text{EO}-\text{Li}^+$ cation coordination in the single-crystal $\text{P}(\text{EO})_3(500):\text{LiCF}_3\text{SO}_3$ structure shows that the $\text{O}2-\text{Li}$ coordination bond is considerably longer than those of $\text{O}1-\text{Li}$ and $\text{O}3-\text{Li}$ ($\text{O}1-\text{Li}1$, $\text{O}2-\text{Li}1$, and $\text{O}3-\text{Li}1$ distances are 2.052(7), 2.468(4), and 2.079(6) Å, respectively). In the $\text{P}(\text{EO})_3(5 \times 10^6):\text{LiCF}_3\text{SO}_3$ structure determined from powder XRD, the ether oxygen $\text{EO}-\text{Li}$ distances were reported to be 1.72(7), 2.38(9), and 2.01(8) Å.^{7b} Further, it was noted that each five-coordinate Li^+ cation is coordinated by three polymer EOs and two oxygen donor atoms (one each from two anions) with each EO coordinated to a single cation. In the single-crystal structure, however, the second electron lone-pair of $\text{O}2$ is directed toward a second Li^+ cation, indicating that an additional very weak coordination bond (3.05 Å) exists (see Supporting Information). The $\text{O}2$ EOs may therefore be considered to be coordinated to two Li^+

* Department of Chemical Engineering & Materials Science.

† Department of Chemistry.

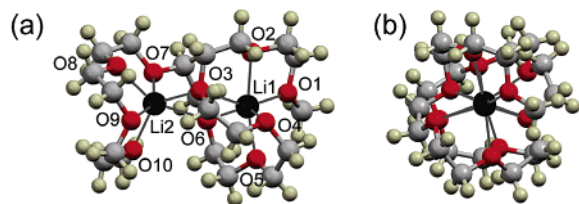


Figure 2. Li^+ cation coordination environment in the single-crystal structure of $\text{P}(\text{EO})_5(500):\text{LiBPh}_4$ (Li, black; O, red). (a) Lateral view and (b) axial view of the $[(\text{EO})_{10}\text{Li}_2]^{2+}$ solvate (anions not shown).

cations. This results in a more symmetrical coordination environment around each six-coordinate Li^+ cation (coordinated by four EOs and two anions) (Figure 1).

The crystal structure of a low molecular weight $\text{P}(\text{EO})_5(500):\text{LiBPh}_4$ phase has also been determined from single crystals (Figure 2).^{11b} A single short PEO chain is helically wrapped around two Li^+ cations. Although this is a 5/1 EO/Li phase, the Li^+ cations actually have weak coordination by a sixth EO (O3–Li1 2.52 Å, O3–Li2 2.10 Å, O6–Li1 2.17 Å, and O6–Li2 2.90 Å). The remaining EOs coordinate a single Li^+ cation with relatively short coordination bonds of 2.01–2.24 Å. This solvate structure may differ from that which forms with high molecular weight PEO. Calorimetric analysis of DSC data used to prepare a PEO– LiBPh_4 phase diagram indicated the formation of a 5.5/1 EO/Li phase.^{4c} The single-crystal structure of $\text{P}(\text{EO})_5(500):\text{LiBPh}_4$ is composed of two unique BPh_4^- anions and a $[(\text{EO})_{10}\text{Li}_2]^{2+}$ dication solvate. The dication has a high amount of thermal disorder. It was thought that there could be PEO chains of various lengths in the structure, but this does not seem to be the case. The dication does not pack well within the cavity bounded by the BPh_4^- anions and appears to squirm in the well-defined pockets. The ends of the PEO chains, in particular, show high thermal motion.

The six-fold cation coordination in $\text{P}(\text{EO})_5(500):\text{LiBPh}_4$ by a single helically wrapped PEO chain is novel. Previously, structures have been reported for $\text{P}(\text{EO})_6:\text{LiX}$ ($X = \text{PF}_6, \text{AsF}_6,$ and SbF_6) phases in which the Li^+ cations are located inside cylinders formed from two PEO chains.^{9d,e} Each chain in these structures adopts a conformation of a half-cylinder with the two halves interlocked around the cations. The uncoordinated anions lie between the cylinders. There are no reported crystal structures of Li^+ cations with six-fold coordination by a single PEO chain. Molecular models of amorphous PEO–LiI electrolytes indicate a preference for three- and six-fold EO coordination to Li^+ cations.¹² The six-fold coordination, however, is predominantly by single chains rather than two chains as found in the $\text{P}(\text{EO})_6:\text{LiX}$ ($X = \text{PF}_6, \text{AsF}_6,$ and SbF_6) phases. Models of glyme– Li^+ cation solvates also indicate that five- and six-fold coordination by a single chain is possible.¹³ The single-chain solvate structure of $\text{P}(\text{EO})_5(500):\text{LiBPh}_4$ may thus be an equally valid model (to the two-chain solvate structures) of PEO– Li^+ cation coordination in amorphous electrolytes. Despite possible differences with high molecular weight PEO structures, the single-crystal structures provide identical insight into the polymer–cation–anion molecular interactions in amorphous polymer electrolytes where ionic conductivity predominates.

Acknowledgment. W.A.H. is indebted to the National Science Foundation and University of Minnesota for the award of Graduate Research Fellowships. Drawings were prepared using the program Mercury.

Supporting Information Available: Crystallographic data, experimental preparations, diagrams of $\text{P}(\text{EO})_5(500):\text{LiCF}_3\text{SO}_3$ and $\text{P}(\text{EO})_5(500):\text{LiBPh}_4$, and calculation of PEO chain length in $\text{P}(\text{EO})_5(500):\text{LiCF}_3\text{SO}_3$ (PDF and CIF). This material is available free of charge via the Internet at <http://pubs.acs.org>.

References

- (1) For instance, see: (a) MacCallum, J. R.; Vincent, C. A., Eds. *Polymer Electrolyte Reviews-1*; Elsevier Applied Science Publ., LTD: New York, 1987. (b) Gray, F. M. *Solid Polymer Electrolytes: Fundamentals and Technological Applications*; VCH Publ.: New York, 1991. (c) Gray, F. M. *Polymer Electrolytes*; The Royal Society of Chemistry: Cambridge, United Kingdom, 1997. (d) Henderson, W. A.; Passerini, S. *Electrochem. Commun.* **2003**, *5*, 575.
- (2) (a) Frech, R.; Chintapalli, S.; Bruce, P. G.; Vincent, C. A. *Chem. Commun.* **1997**, 157. (b) Mao, G.; Saboungi, M.-L.; Price, D. L.; Armand, M. B.; Howells, W. S. *Phys. Rev. Lett.* **2000**, *84*, 5536. (c) Mao, G.; Saboungi, M.-L.; Price, D. L.; Badyal, Y. S.; Fischer, H. E. *Europhys. Lett.* **2001**, *54*, 347.
- (3) (a) Andreev, Y. G.; Bruce, P. G. *Electrochim. Acta* **2000**, *45*, 1417. (b) Andreev, Y. G.; Bruce, P. G. *J. Phys.: Condens. Matter* **2001**, *13*, 8245.
- (4) For instance, see: (a) Robitaille, C. D.; Fauteux, D. *J. Electrochem. Soc.* **1986**, *133*, 315. (b) Vallée, A.; Besner, S.; Prud'homme, J. *Electrochim. Acta* **1992**, *37*, 1579. (c) Besner, S.; Vallée, A.; Bouchard, G.; Prud'homme, J. *Macromolecules* **1992**, *25*, 6480.
- (5) (a) Iwamoto, R.; Saito, Y.; Ishihara, H.; Tadokoro, H. *J. Polym. Sci., Part A-2* **1968**, *6*, 1509. (b) Yokoyama, M.; Ishihara, H.; Iwamoto, R.; Tadokoro, H. *Macromolecules* **1969**, *2*, 184. (c) Chatani, Y.; Okamura, S. *Polymer* **1987**, *28*, 1815. (d) Chatani, Y.; Fujii, Y.; Takayanagi, T.; Honma, A. *Polymer* **1990**, *31*, 2238.
- (6) (a) Parker, J. M.; Wright, P. V.; Lee, C. C. *Polymer* **1981**, *22*, 1307. (b) Hibma, T. *Solid State Ionics* **1983**, *9/10*, 1101.
- (7) (a) Lightfoot, P.; Mehta, M. A.; Bruce, P. G. *J. Mater. Chem.* **1992**, *2*, 379. (b) Lightfoot, P.; Mehta, M. A.; Bruce, P. G. *Science* **1993**, *262*, 883. (c) Lightfoot, P.; Nowinski, J. L.; Bruce, P. G. *J. Am. Chem. Soc.* **1994**, *116*, 7469. (d) Thomson, J. B.; Lightfoot, P.; Bruce, P. G. *Solid State Ionics* **1996**, *85*, 203.
- (8) (a) Andreev, Y. G.; Lightfoot, P.; Bruce, P. G. *J. Appl. Crystallogr.* **1997**, *18*, 294. (b) Andreev, Y. G.; Bruce, P. G. *J. Chem. Soc., Dalton Trans.* **1998**, 4071.
- (9) (a) Andreev, Y. G.; Lightfoot, P.; Bruce, P. G. *J. Chem. Soc., Chem. Commun.* **1996**, 2169. (b) Andreev, Y. G.; MacGlashan, G. S.; Bruce, P. G. *Phys. Rev. B* **1997**, *55*, 12011. (c) MacGlashan, G. S.; Andreev, Y. G.; Bruce, P. G. *J. Chem. Soc., Dalton Trans.* **1998**, 1073. (d) MacGlashan, G. S.; Andreev, Y. G.; Bruce, P. G. *Nature* **1999**, *398*, 792. (e) Gadjourova, Z.; Martín y Marero, D.; Andersen, K. H.; Andreev, Y. G.; Bruce, P. G. *Chem. Mater.* **2001**, *13*, 1282. (f) Martin-Litas, I.; Andreev, Y. G.; Bruce, P. G. *Chem. Mater.* **2002**, *14*, 2166.
- (10) Henderson, W. H. Ph.D. Thesis; University of Minnesota, 2002.
- (11) Crystal data for (a) $\text{P}(\text{EO})_5(500):\text{LiCF}_3\text{SO}_3$: FW = 288.54, $\text{C}_7\text{H}_{12.33}\text{F}_3\text{LiO}_6\text{S}$, colorless, blocks (0.44 × 0.20 × 0.20 mm), monoclinic, space group $P2_1/n$, $a = 10.0678(16)$ Å, $b = 8.5275(14)$ Å, $c = 14.399(2)$ Å, $\beta = 96.023(3)^\circ$, $V = 1229.4(3)$ Å³, $\rho_{\text{calc}} = 1.559$ mg m⁻³, $Z = 4$, $2\theta_{\text{max}} = 25.04^\circ$, Mo K α radiation ($\lambda = 0.71073$ Å), $T = 173(2)$ K. X-ray data were collected using a Bruker SMART CCD area detector diffractometer, and the structure was solved via direct methods using SHELXS-97 (SHELXTL-Plus V 5.10, Bruker Analytical X-ray Systems, Madison, WI, 1998). Full-matrix least-squares refinement using SHELXL-97 converged with $R = 0.0367$ and $wR^2 = 0.0863$ for 2168 independent reflections with $I > 2\sigma(I)$ and 237 parameters and 27 restraints. (b) $\text{P}(\text{EO})_5(500):\text{LiBPh}_4$: FW = 1094.84, $\text{C}_{68}\text{H}_{82}\text{B}_2\text{LiO}_{10}$, colorless, blocks (0.22 × 0.14 × 0.08 mm), monoclinic, space group $P2_1/n$, $a = 12.5349(15)$ Å, $b = 36.295(4)$ Å, $c = 13.0899(15)$ Å, $\beta = 91.276(3)^\circ$, $V = 5953.8(12)$ Å³, $\rho_{\text{calc}} = 1.221$ mg m⁻³, $Z = 4$, $2\theta_{\text{max}} = 25.06^\circ$, Mo K α radiation ($\lambda = 0.71073$ Å), $T = 173(2)$ K. X-ray data were collected using a Bruker SMART CCD area detector diffractometer, and the structure was solved via direct methods using SHELXS-97. Full-matrix least-squares refinement using SHELXL-97 converged with $R = 0.0956$ and $wR^2 = 0.3040$ for 10 372 independent reflections with $I > 2\sigma(I)$ and 741 parameters and 736 restraints. Anal. Calcd for $\text{P}(\text{EO})_5(500):\text{LiBPh}_4$: C, 74.6; H, 7.5. Found: C, 71.75; H, 7.85.
- (12) (a) Müller-Plathe, F.; van Gunsteren, W. F. *J. Chem. Phys.* **1995**, *103*, 4745. (b) Borodin, O.; Smith, G. D. *Macromolecules* **1998**, *31*, 8396.
- (13) Johansson, P.; Tegenfeldt, J.; Lindgren, J. *Polymer* **1999**, *40*, 4399.

JA036535K